Convergence of Clinically Relevant Manipulations on Dopamine-Regulated Prefrontal Activity Underlying Stress-Coping Responses

Supplemental Information

SUPPLEMENTAL METHODS AND MATERIALS

All experiments were conducted in accordance with procedures established by the administrative panels on laboratory animal care at the University of California, San Francisco.

Mouse lines, viral vectors and viral targeting/expression: For all experiments using wildtype mice, C57BL/6J derived lines were bred in house or ordered from Jackson Laboratories or Charles River. Dominant negative Disc1 mutant mice were generated by crossing B6-CamKII::TtA (JAX: 00310) mice with tetO-DISC1dn (JAX: 008790) to yield mice expressing dominant negative DISC1 in neocortical pyramidal cells (1). For slice experiments, wildtype or Disc1 mutant mice at P26-P35 were injected with 4x 150 nl of AAV5-CaMKII-GCaMP6f (UPenn Virus Core) at 4 depths (dorso-ventral (DV): -2.0, -2.25, -2.50, -2.75) at the following (millimeters relative to bregma) coordinates for mPFC: 1.7 anterior-posterior (AP) and 0.3 mediolateral (ML). We allowed between 2-3 weeks for viral expression before sacrificing mice and cutting live prefrontal brain slices for calcium imaging (imaged mice were between 6-8 weeks of age when sacrificed). Mice used in social defeat experiments were slightly older to ensure full surgical recovery before defeats and adequate social aggression between males. These were injected as above at P35-42 and were imaged at 10-11 weeks of age. For optogenetics targeting VTA-mPFC projections, mice were heterozygous TH::Cre (line FI12; www.gensat.org) and a mixture of male and female mice were used. Optogenetics experiments targeting D2R+ mPFC neurons used male heterozygous D2::Cre mice (line ER44; www.gensat.org). Cre-dependent expression was driven using previously described adeno associated virus (AAV5) containing DIO-ChR2-eYFP or DIO-eYFP expressed under the synapsin promoter (2). We stereotaxically injected 1.0 µl of 4-10 x 10^{12} vg/ml virus into right VTA of P56-70 TH::Cre mice or 600 nl into the right mPFC using methods described previously (2,3). Coordinates relative to bregma in millimeters were −2.75 AP, ±0.5 ML, and −4.5 DV for all experiments targeting VTA and +1.7 AP, ±0.3 ML, and −2.5 DV for experiments targeting D2R+ neurons in mPFC . At least 8 weeks were allowed for expression and trafficking to VTA terminals in mPFC. For Drd2 deletion experiments, mice were Drd2loxP/loxP homozygous (JAX: 020631) (4). Localized deletion of Drd2 in mPFC was accomplished using AAV5 containing Cre-mCherry or mCherry expressed under synapsin promoter (UPenn Virus Core). Coordinates relative to bregma were +1.7 AP, ±0.3 ML, and −2.5 DV and we injected 750 nl of 3-7 x 10^{12} vg/ml virus bilaterally in P56-P70 wildtype mice of either sex. At least 4 weeks were allowed for expression/deletion before proceeding with behavior experiments.

For all optogenetics experiments, mice were implanted with a 200 µm diameter, 0.22NA fiber optic cannulae (Doric Lenses) over right mPFC (1.7 AP, 0.35 ML, -2.25 DV). Implants were affixed onto the skull using Metabond dental cement (Parkell). Targeting of viral constructs/cannulas, and expression of channelrhodopsin2 (ChR2) in prefrontal terminals were confirmed via histology without immunostaining.

Slice calcium imaging experiments: In all cases, 350-micron thick live coronal slices were prepared from mice between 2-4 weeks after injection. Slice preparation followed our previously described protocol (5), briefly, slices were cut and incubated for 10 minutes in N-methyl-D-glucamine (NMDG)-based recovery solution before being transferred to ACSF for the remainder of the recovery period. The NMDG-based solution was maintained at 32C and used to maintain the overall health of adult slices to ensure sufficient activity for analysis. Prior to imaging, slices were moved from the recovery solution to one with 2 µM carbachol to promote adequate activity in prefrontal microcircuits during imaging. For details see (5) GCaMP6f imaging was performed on an Olympus BX51 upright microscope with a 20x

1.0NA water immersion lens, 0.5x reducer (Olympus, Tokyo, Japan), and ORCA-ER CCD Camera (Hamamatsu Photonics, Hamamatsu, Japan). Illumination was delivered using a Lambda DG4 arc lamp (Sutter Instruments, Novato, California). Light was delivered through a 472/30 excitation filter, 495 nm single-band dichroic, and 496 nm long pass emission filter (Semrock, Rochester, New York). All recordings were at 32.5 +/- 1C. All movies that were analyzed consisted of 36,000 frames acquired at 10 Hz (1 hour) with 4 X 4 sensor binning yielding a final resolution of 256 X 312 pixels. For D2 and D1R stimulation experiments, baseline activity was imaged for 20 minutes, at which point the solution was switched to one containing 10 μM quinpirole (Sigma) or 10 μM SKF-38393 (Sigma) to stimulate dopamine D2 and D1 receptors respectively. For D2R antagonist experiments, slices were pre-incubated and maintained in solutions containing 10 μM sulpiride (Sigma) for the duration of imaging, 10 μM quinpirole was added at 20 minutes as described above. Light power during imaging was 100 to 500 $\mu W/mm^2$. The Micro Manager software suite (v1.4, National Institutes of Health, Bethesda, Maryland) was used to control all camera parameters and acquire movies. Subtle drift in x or y dimensions was corrected using an image alignment plugin for ImageJ software package, called cvMatch_Template, which effectively eliminated drift (6). Any movies with significant drift that could not be corrected or that lacked significant amounts of activity were excluded from further analysis. Cortical layers were clearly delineated by GCaMP expression and the bulk of infected neurons were localized to layer 5, where we focused the center of our imaging window. Slices imaged were localized to mPFC, primarily prelimbic and infralimbic regions (**Figure S1**).

Signal Extraction and correlations: All analyses and signal extraction was performed using MATLAB (Mathworks) and methods used for performing signal extraction are identical to our previous slice calcium imaging work. We used a PCA/ICA approach modified from the published CellSort 1.1 toolbox (7) as previously described (5,8), detecting signals from between 80-100 ROIs per slice (presumed neurons). In brief, the baseline fluorescence function, F0, was calculated for every trace using the mode of the kernel density estimate over a 100s rolling window, implemented via the MATLAB function ksdensity following the procedure outlined in (9). All signal traces shown represent normalized versions of the (F-F0)/F0 trace. Raw fluorescence correlations were calculated based on these traces, as described in the text and previously (10). In brief, we sought to summarize the patterns of local microcircuit activity using the pattern of correlations between activity in different neurons. Inter-neuronal correlations were computed as the normalized vector dot product between a time series of GCaMP signals and a time series of derivatives (corresponding to a different neuron). In addition to correlation, we also calculated a p-value for how well activity in one ROI predicts fluctuations in the other. Comparisons were made between conditions for positive correlations with a p-value less than 0.01 to ensure we were looking at meaningful correlations and excluding 'noise' and because significant positive correlations were most consistently modulated across experimental conditions. We used shuffled datasets (in which each trace has been shifted over by a random amount) or scrambled datasets (in which new traces were formed from random linear combinations of the original traces) to show that this algorithm detects statistically-meaningful correlations, i.e., correlations not present in shuffled/scrambled datasets (10). We also created simulated data composed of nominally independent signals contaminated by shared background fluorescence, correlations between signals are markedly large in magnitude than correlations between signals and their derivatives. Correlations calculated from real data followed a very similar distribution (10).

In vivo pharmacology: For slice experiments combined with an in vivo pharmacologic manipulation (fluoxetine or ketamine), drugs were diluted in 0.9% sterile saline and injected intraperitoneally. Mice treated with fluoxetine were administered daily doses at 20 mg/kg every day for 3 weeks. Mice were imaged as saline and fluoxetine treated littermate pairs on the same day, in counterbalanced order. For ketamine experiments, we first tested a range of ketamine doses (3, 10 and 25 mg/kg) alongside saline controls injected intraperitoneally (7 week old wildtype mice). Mice were tested 24 hours later using the TST in order to assess antidepressant-like, dose-response relationships (**Figure S3**). Based on this validation dose-response curve, 10 mg/kg was selected as the dosage of ketamine used for subsequent slice experiments as this had the maximal effect on reduction of immobility in the TST. We subsequently confirmed an antidepressant-like effect for ketamine at this dose in a cohort of animals

that included those used for imaging. For ketamine slice experiments, littermate pairs were injected together – one with 10 mg/kg ketamine and one with saline as a control – and slices were cut and imaged from both mice the next day (~24 hours post-injection).

Behavior experiments: Mice were housed under standard 12-h light/dark cycles, and all experiments were performed during the light portion of the cycle. After sufficient time for surgical recovery and viral expression, mice underwent multiple rounds of habituation. The testing room was illuminated at 150 lux, and mice were first habituated to the behavioral testing area for at least 30 minutes prior to the beginning of any further handling each day. Mice were then habituated to touch with at least 3 days of handling for ~5 min each day, followed by 1–2 days of habituation to the optical tether in their home cage for 10 min. All behavior video was captured via a USB webcam (Logitech) connected to a computer running ANY-maze (Stoelting) which was used to track the position of the mouse during behavior. Mice were randomly assigned to a viral condition and the experimenter was blinded to the mouse's virus assignment during all subsequent behavioral assessment or analyses.

Tail suspension test (TST): TST mice were suspended by taping their tail to a bar ~12 inches above the tabletop, within 4 inch wide stalls of a custom apparatus constructed for this purpose. A 1.5 ml microcentrifuge tube was cut and placed over the tail base to prevent the mouse from climbing its tail during testing. Per standard protocols, and to ensure a stable base level of struggling, the first 2 minutes of the TST was not analyzed. The TST for optogenetics experiments was 14 minutes in duration and only one mouse was run at a time. Optogenetic stimulation was delivered in 4x, 3 minute blocks (OFF-ON-OFF-ON) with stimulation parameters as per below. For all other experiments, the TST was 10 minutes in duration and up to 4 mice were run simultaneously in separate stalls where they were not visible to each other. The apparatus was thoroughly cleaned between uses. TST videos for VTA terminal optogenetics were analyzed manually on a per minute basis by an experimenter that was blinded to the conditions being tested and using an established method (11). For TST videos from Drd2 deleted mice and D2R-Cre optogenetic stimulation, we developed an unbiased, automated analysis algorithm using Matlab, that allowed us to quantify not only total duration of struggling, but also the number and duration of individual struggling episodes. To do this, we developed a custom analysis process where videos were analyzed using ANY-maze software (Stoelting) to track lateral movement of a point at the base of the mouse's tail during the TST. Several points of tracking were assessed, but tailbase movements most faithfully captured distinct episodes. A custom Matlab script was developed which converted x/y-tracking coordinates to a lateral velocity value for each frame and automatically set a minimum velocity threshold for mobility episodes. Thresholds were established for each dataset using a classifier developed for this purpose and trained on human annotated data. Only sustained, effortful increases in velocity (>3s) were categorized as struggling and additional Matlab code was used to analyze the number and duration of individual episodes, and compare between conditions.

Open field (OF): OF testing was conducted in a standard sized arena (40x40cm), with a height of 30cm. Video was collected from above and subsequent analysis was done using built-in ANY-maze tracking. Open field testing was 8 minutes in duration and mouse was placed by hand into the lower right corner of the apparatus. Optogenetic stimulation was delivered in 4x, 2 minute blocks (OFF-ON-OFF-ON) with stimulation parameters as per below. Total distance traveled in the apparatus, total or on a per minute basis, was analyzed as a measure of overall activity level.

Social Defeat Stress: Social defeat stress experiments were conducted consistent with standardized protocols for this procedure (12). Retired, singly housed CD-1 male breeder mice (Charles River; 4-6 months of age) were screened for adequate aggression prior to starting protocol. Male C57 BL/6 mice between 5-6 weeks of age were injected with GCaMP virus as per above and were allowed 2 weeks to recover after surgery before starting defeat protocol. Mice were exposed to 10 minutes of defeat from CD-1 aggressor mice, followed by 6-8 hours of exposure to the aggressor in a cage divided by a perforated plexiglass barrier for 10 consecutive days. Aggressor mice were rotated each day to prevent habituation and the quantity and quality of aggressive episodes was monitored to ensure even exposure to defeat. Control mice were exposed similarly, but to cagemates instead of aggressor mice.

24 hours after the last defeat, mice were tested for social interaction in a standard open field arena in which a completely novel CD-1 mouse was secured inside a wire-mesh cup. Mice were briefly exposed to the CD-1 mouse, followed by exposure to an empty cup alone (3 minute each, separated by 30s). A social interaction zone around the cup was established and social interaction ratio (SI ratio) calculated as time spent in the interaction zone with the CD-1 mouse divided by without. SI ratios for defeated mice roughly segregated into two clusters, those within the range of control mice were defined as 'resilient' and those much lower in a clearly dissociable cluster, as 'susceptible' for the purposes of our experiment. We then cut slices from littermate mice within 72 hours of the social interaction test as per protocol described above. Resilient and susceptible mice were imaged on the same day in counterbalanced order to ensure the most rigorous comparison and no defeat controls were imaged over subsequent days (within one week of defeated mice).

Optogenetic stimulation protocols: For optogenetic stimulation during behavior, light stimulation was delivered via a fiber optic cable fed through a commutator (Doric Lenses) and attached to a 100 mW, 473 nm laser (OEM). For dopamine terminal stimulation, the laser was driven with a pulse generator using two protocols: In the tonic protocol a 5 Hz train of 4 ms pulses was used while in the phasic protocol 500 ms bursts of 50 Hz 4 ms pulses were delivered every 5 seconds. Each protocol delivers the exact same number of pulses and total light power during each 5 seconds of stimulation. For D2R+ neuron stimulation, the laser was driven by a pulse generator which was triggered via TTL pulses from a computer running Anymaze software. Anymaze software was custom configured to track movements at the tailbase during the TST. A narrow zone was aligned over the tailbase at rest. No movement outside that zone for at least 3 seconds was considered immobility and triggered a continuous 20 Hz train of 4 ms pulses. Any movement outside that zone (i.e., struggling) immediately terminated stimulation until immobility criteria were met again. The total light power delivered during a pulse was 5 mW.

Statistics: Unless otherwise specified, nonparametric tests or ANOVA was used to assess significance. Statistics were calculated using custom MATLAB code or Graphpad Prism. All statistical parameters, including test statistics, correction for multiple comparisons, and sampling of repeated measurements are stated in the main figure legends. Error bars represent ±SEM. The code and data used to generate and support the findings of this study are available from the corresponding author upon reasonable request.

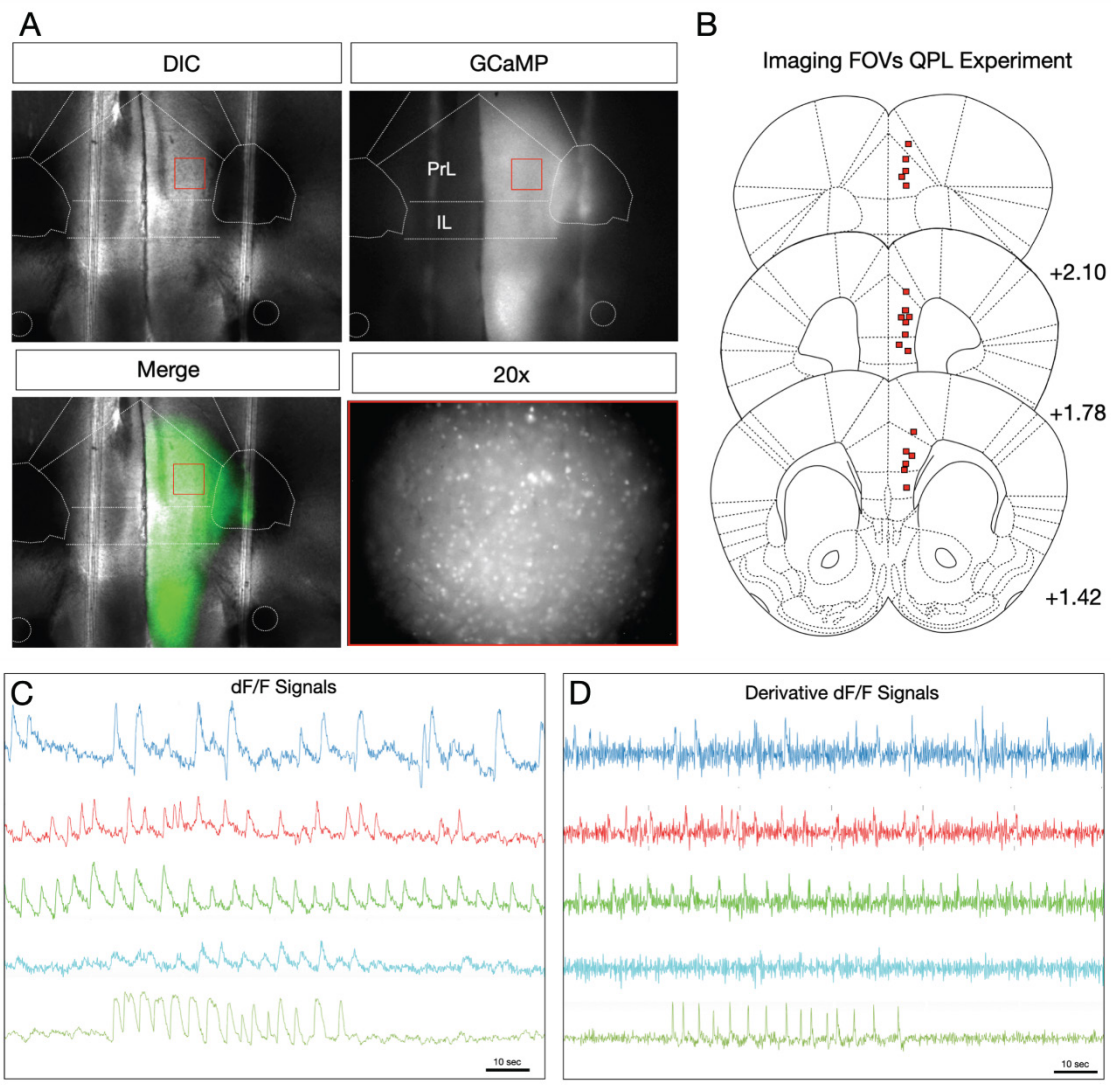

Supplementary Figure S1: Localization of imaging windows for slices used in slice calcium imaging experiments.

(A) Low magnification images of an example prefrontal slice used for experiments. DIC and GCaMP fluorescence images are shown with prelimbic (PrL) and infralimbic (IL) cortices outlined, where the majority of imaging windows (e.g., red box) were placed. An example 20x image of prefrontal cells visualized in deep layer PrL are shown. **(B)** Approximate locations of all imaging fields of view (FOVs) are shown for the slices used in the quinpirole (QPL) imaging experiment shown in main figure 1. Imaging windows for all other slice experiments are similar. Coordinates are A/P relative to bregma. **(C)** Examples of dF/F0 signals are shown, while **(D)** shows the corresponding derivative signals, calculated as described in the manuscript.

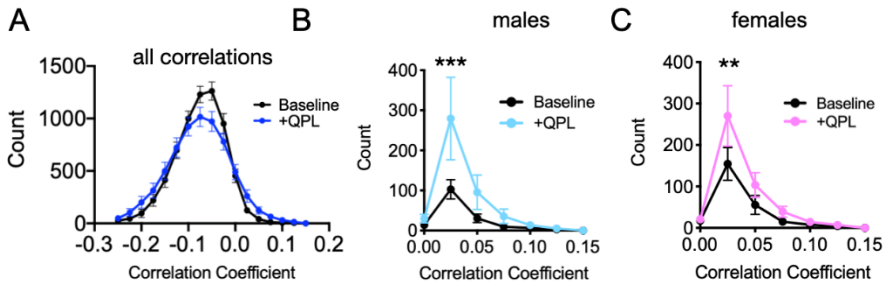

Supplementary Figure S2: Plotting correlations for specific comparisons.

(**A**) Quantification of all correlations between every cell-pair in quinpirole experiment showing substantial overlap between conditions. (**B**) Quantification of significant positive correlations only for male mice in the quinpirole experiment, baseline vs. quinpirole (n=11 slices) [$F_{Interaction}(6,140)=2.038$, $P=0.0646$, $F_{Drug}(1,140)=6.185$, $P=0.0141$], 2-way ANOVA with Sidak post-hoc test. (**C**) Quantification of significant positive correlations only for female mice in the quinpirole experiment, baseline vs. quinpirole (n=8 slices) [$F_{Interaction}(6,98)=1.432$, $P=0.210$, $F_{Drug}(1,98)=4.654$, $P=0.0334$], 2-way ANOVA with Sidak post-hoc test. Statistics represent mean±SEM, $^{**}P<0.01$, $^{***}P<0.001$.

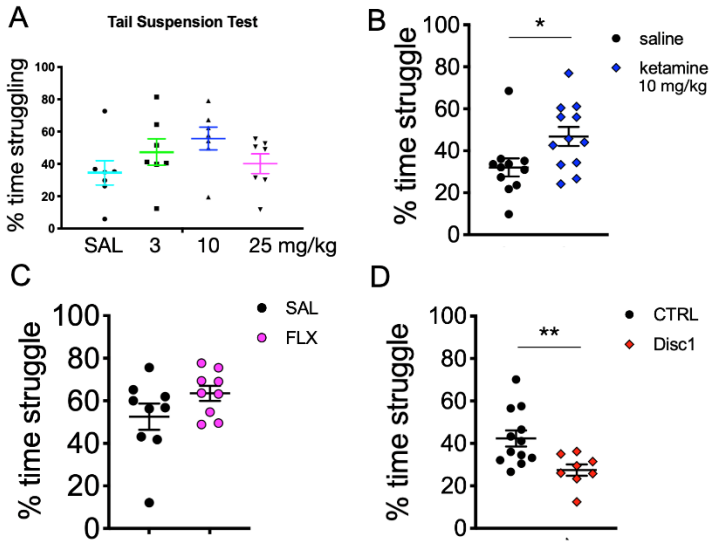

Supplementary Figure S3: Tail suspension test data for manipulations

(**A**) Dose-response curve for determining antidepressant dose of ketamine. (**B**) Quantification of TST data for saline (n=11) vs. ketamine 10 mg/kg (n=12), unpaired t-test [t=2.333, df=21, p=0.0296]. (**C**) Quantification of TST data for saline (n=9) vs. fluoxetine (n=9), unpaired t-test [t=1.551, df=16, p=0.141]. (**D**) Quantification of TST data for control (n=12) vs. Disc1-DN (n=8), unpaired t-test [t=2.882, df=18, p=0.0099]. Statistics represent mean±SEM, **P*<0.05, ***P*<0.01.

SUPPLEMENTAL REFERENCES

1. Pletnikov M V, Ayhan Y, Nikolskaia O, Xu Y, Ovanesov M V, Huang H, *et al.* (2008): Inducible expression of mutant human DISC1 in mice is associated with brain and behavioral abnormalities reminiscent of schizophrenia. *Mol Psychiatry* 13: 173–86, 115.
2. Ellwood IT, Patel T, Wadia V, Lee AT, Liptak AT, Bender KJ, Sohal VS (2017): Tonic or phasic stimulation of dopaminergic projections to prefrontal cortex causes mice to maintain or deviate from previously learned behavioral strategies. *J Neurosci* 37: 8315–8329.
3. Gee S, Ellwood I, Patel T, Luongo F, Deisseroth K, Sohal VS (2012): Synaptic activity unmasks dopamine D2 receptor modulation of a specific class of layer V pyramidal neurons in prefrontal cortex. *J Neurosci* 32: 4959–71.
4. Bello EP, Mateo Y, Gelman DM, Noaín D, Shin JH, Low MJ, *et al.* (2011): Cocaine supersensitivity and enhanced motivation for reward in mice lacking dopamine D2 autoreceptors. *Nat Neurosci* 14: 1033–1038.
5. Luongo FJ, Horn ME, Sohal VS (2016): Putative microcircuit-level substrates for attention are disrupted in mouse models of autism. *Biol Psychiatry* 79: 667–675.
6. Tseng Q, Wang I, Duchemin-Pelletier E, Azioune A, Carpi N, Gao J, *et al.* (2011): A new micropatterning method of soft substrates reveals that different tumorigenic signals can promote or reduce cell contraction levels. *Lab Chip* 11: 2231–2240.
7. Mukamel EA, Nimmerjahn A, Schnitzer MJ (2009): Automated Analysis of Cellular Signals from Large-Scale Calcium Imaging Data. *Neuron* 63: 747–760.
8. Luongo FJ, Zimmerman C, Horn ME, Sohal VS (2016): Correlations between prefrontal neurons form a small world network that optimizes the generation of multineuron sequences of activity. *J Neurophysiol* jn.01043.2015.
9. O'Connor DH, Peron SP, Huber D, Svoboda K (2010): Neural activity in barrel cortex underlying vibrissa-based object localization in mice. *Neuron* 67: 1048–1061.
10. Lee AT, Cunniff MM, See JZ, Wilke SA, Luongo FJ, Ellwood IT, *et al.* (2019): VIP Interneurons Contribute to Avoidance Behavior by Regulating Information Flow across Hippocampal-Prefrontal Networks. *Neuron* 102: 1223-1234.e4.
11. Can A, Dao DT, Terrillion CE, Piantadosi SC, Bhat S, Gould TD (2011): The tail suspension test. *J Vis Exp* e3769.
12. Golden SA, Covington HE, Berton O, Russo SJ (2011): A standardized protocol for repeated social defeat stress in mice. *Nat Protoc* 6: 1183–1191.